Sensors and Actuators A 148 (2008) 299–305

Contents lists available at ScienceDirect

Sensors and Actuators A: Physical

journal homepage: www.elsevier.com/locate/sna

High temperature operation of multi-watt, axial-flux, permanent-magnet microgenerators

Florian Herrault*, David P. Arnold[1], Iulica Zana[2], Preston Galle, Mark G. Allen

School of Electrical and Computer Engineering, Georgia Institute of Technology, Atlanta, GA 30332, USA

ARTICLE INFO

Article history:
Received 26 March 2008
Received in revised form 23 May 2008
Accepted 15 July 2008
Available online 25 July 2008

Keywords:
Electric machines
Magnetic losses
MEMS
Permanent-magnet generators
Thermal factors

ABSTRACT

This paper presents the characterization and modeling of a permanent-magnet (PM) microgenerator operating at high temperatures. Due to the thermal dependence of the relevant properties of the conductor and magnetic materials, degradation of the output electrical power with increased temperature is expected. Each material of the PM microgenerator is magnetically or electrically characterized up to 375 °C. For a rotor designed for high temperature operation using SmCo magnets, 2.7 W of DC power has been obtained at 100 °C and 210,000 rpm, which is a 35% drop as compared to the output power at room temperature. This result is in good agreement with theory. Calculations showed that this PM generator is capable of 2.4 W of DC output power at an operating temperature of 300 °C if the rotational speed is increased up to the 300,000 rpm, as achieved with previous room temperature devices. This work demonstrates that MEMS-based permanent-magnet microgenerators are good candidates as a component of a heat-engine-driven electrical power generation system.

1. Introduction

The power requirements of modern electronic devices are rapidly outpacing the power density and energy of the best batteries. This has led to the development of small-scale, watt-level, electrical power sources intended for power electronics. Accordingly, heat-engine-driven MEMS-based systems are very attractive, and consist of a cm-scale gas-fueled turbine engine [1], and an electrical generator [2–4] as the chemical-to-mechanical, and mechanical-to-electrical converters, respectively.

Recently, there has been much work in the development of microscale mechanical-to-electrical generators as essential components of these heat-engine-driven electrical power sources for portable electronics. However, in such compact systems, the generators must function in the relatively high temperature environment adjacent to the heat engine. Although a number of small-form-factor microgenerator systems ultimately intended for integration with heat engines have been presented [2–4], less attention has been paid to their high temperature performance. Indeed, microgenerators typically use low temperature magnetic materials [2,3] to obtain better performance rather than high temperature compatible magnetics. Performance requirements are further exacerbated by the compact nature of these microsystems and the difficulties involved in maintaining large internal thermal gradients.

This paper reports the high temperature operation of axial-flux, permanent-magnet (PM) microgenerators. These devices are capable of delivering watt-level DC power to an external load at an operating temperature of 300 °C. First, the microgenerator design is presented, and considerations on the temperature range of operation of these microgenerators integrated with heat engines are detailed. The magnetic materials used in the PM microgenerators are characterized up to 375 °C, and the temperature dependence of the electroplated copper windings is also investigated. A phenomenological model is introduced to express the power degradation based on the measured material properties as a function of temperature. Finally, measurements of electrical power for several microgenerators at high temperatures are reported and discussed.

2. Generator design

As shown in Fig. 1, previously reported high-speed rotors [5] and optimized stators [4,6] are used for these high temperature experiments. The generators are three-phase, eight-pole, axial-flux, synchronous machines, each consisting of copper stator windings [7,8], and a multi-pole permanent-magnet rotor [9]. An external air-driven turbine spins the PM rotor, which creates a time-varying

* Corresponding author.
E-mail address: fh59@mail.gatech.edu (F. Herrault).
[1] Now with Department of Electrical and Computer Engineering, University of Florida, Gainesville, FL 32611, USA.
[2] Now with Western Digital Corp., Fremont, CA 94539, USA.

0924-4247/$ – see front matter © 2008 Elsevier B.V. All rights reserved.
doi:10.1016/j.sna.2008.07.012

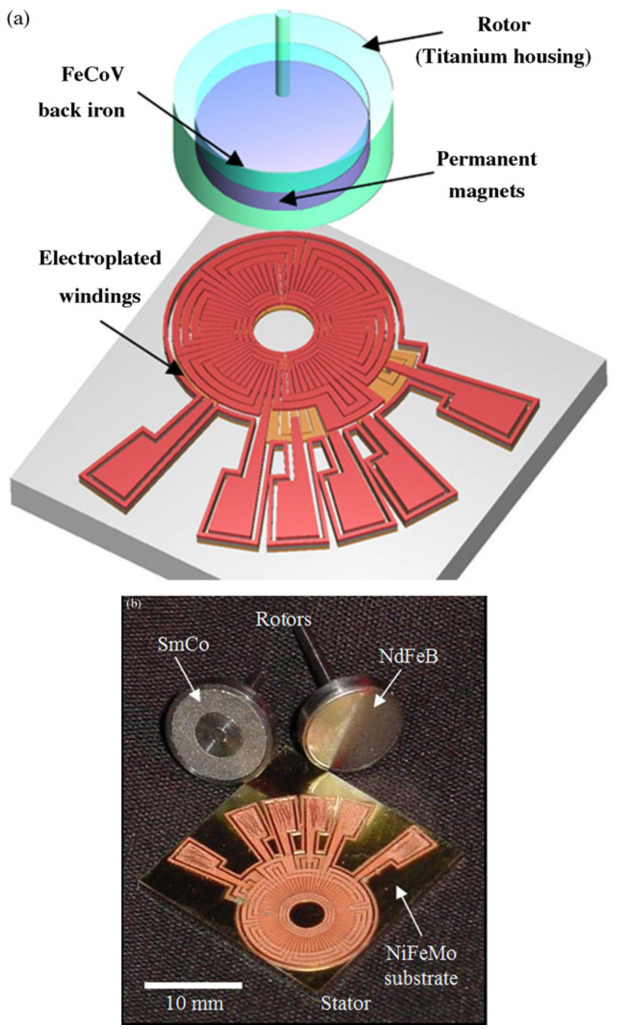

Fig. 1. Optimized winding geometry stator and rotors: (a) Three-dimensional (3-D) rendering, and (b) 3-D view of the stator and two rotors with different permanent-magnet materials.

magnetic flux. As a result, AC voltages are induced in the coils. When a load resistance is connected to the windings, electrical power is generated.

The stator is fabricated using conventional microfabrication approaches, and consists of two layers of electroplated copper coils with an SU-8 epoxy interlayer dielectric on top of a ferromagnetic NiFeMo (moly-permalloy) substrate. The stator is designed as an eight-pole, three-turn/pole device and exhibits a resistance per phase of approximately 170 mΩ. Simulations have previously been performed and have shown that this configuration yields the highest output power [4]. Per phase, open-circuit voltages are varying in the 0.5–2V_{RMS} range at room temperature. The rotor includes a ferromagnetic material (FeCoV – Hiperco 50) to serve as a back iron, and a permanent-magnet material. Rotors operate at speeds of up to 400,000 rpm.

3. Temperature considerations of small-scale gas engines

Such electromagnetic generators are intended for integration with heat-engine-driven, high-speed turbine systems. Fréchette and coworkers are developing a MEMS-based, Rankine cycle steam turbine [10,11]. Their current efforts are focused on the development of the high-speed rotating system, but considerations on the electrical generator have also been introduced. It must withstand high rotational speeds (rotor tip velocity of 100’s of m/s), and sustain high temperatures. The rotor should reside at an average of the minimum and maximum cycle temperatures, which corresponds to temperatures varying between 200 and 400 °C.

Stevens et al. discussed several design issues of a fuel-based micropower generator [12]. To overcome the temperature-related issues in the magnetic generator, the permanent magnets must be integrated at the lowest temperature side of the turbine (i.e., compressor side), and extra cooling should be provided through passing air across the magnets. The PM generator is located in an environment with temperatures varying between 200 and 300 °C. To surmount the detrimental effects caused by high temperatures, and because the output power delivered by the machine varies as the square of the rotor speed, high rotational speeds are required in order to fabricate microgenerators with high power density capabilities.

As a result of the temperature-related considerations reported by Fréchette and Stevens with regards to the integration of PM microgenerators with heat engines, the fabricated devices must be able to operate at temperatures around 200–300 °C. Detrimental temperature-dependent material effects consist of increased winding resistance and decreased magnetic properties, including decreases to both permanent-magnet remanence, and ferromagnetic saturation magnetization. Consequently, the PM microgenerators and their temperature-dependent materials have been characterized in this temperature range.

4. High temperature characterization

4.1. Magnetic characterization

The thermal dependences of the small-scale magnetics have been investigated using a Vibrating Sample Magnetometer (VSM) with an integrated furnace. The temperature ramp is set at 25 °C per 1.5 min. For each measurement, the system is stabilized for a few minutes before recording any data. Both PM materials and ferromagnetic materials in the geometries and size scales of interest have been tested. SmCo and NdFeB PM materials are 0.5 mm thick. FeCoV and NiFeMo back iron materials are of a thickness of 1 mm.

Both, SmCo and NdFeB are characterized as possible permanent-magnet materials. Although SmCo has a lower room temperature remanence (B_r = 11.5 kG) compared to NdFeB (B_r = 13.9 kG), it possesses a much higher Curie temperature ($T_c \sim 800$ °C) and maximum operating temperature ($T_{max} \sim 300$ °C) as compared to NdFeB ($T_c \sim 300$ °C, $T_{max} \sim 100$ °C). At high temperatures, SmCo will likely be preferred. However, high rotational speeds or directed airflow may provide sufficient cooling to use the better performing but more temperature-sensitive NdFeB magnets at moderate temperatures.

The temperature-dependent remanence of microscale rotor magnets have been experimentally determined as depicted in Fig. 2. These results for the different materials are presented as normalized to their respective room temperature values. Neglecting any potential cooling effects due to high rotational speeds of the PM rotors, these microscale NdFeB magnets cannot be used above approximately 150 °C due to a nearly complete remanence loss at high temperatures. From the experimental data, an approximate curve fit for the temperature dependence for microscale permanent magnets is defined by

$$B_r(T) = B_{r(25\,^\circ C)} \times (1 + \alpha_{PM} \times (T - 25)) \quad (1)$$

where $B_r(T)$ is the measured remanence of the permanent-magnet material at a temperature T in °C and α_{PM} is a linear coefficient

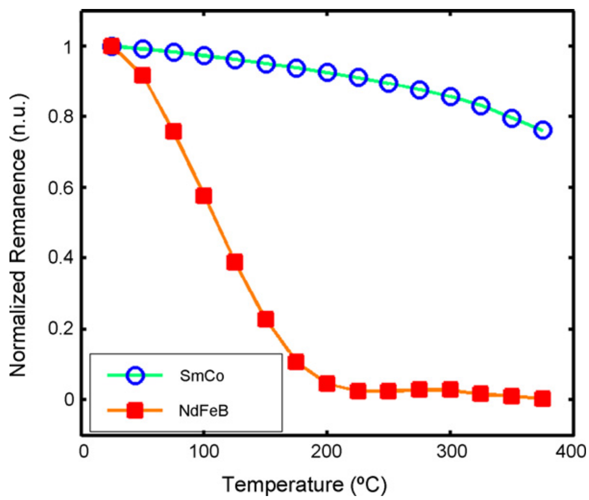

Fig. 2. Measured remanence of saturated SmCo and NdFeB magnetic rotors as a function of temperature, normalized to their respective measured room temperature remanences.

of temperature dependence. Hence, the coefficient of temperature dependence for microscale NdFeB magnets (α_{NdFeB}) is about $-0.6\%\,^{\circ}\mathrm{C}^{-1}$ over a low range of temperatures (25–100 °C). This coefficient is much higher than macroscale NdFeB permanent magnets ($\sim$0.1% $^{\circ}\mathrm{C}^{-1}$) [13]. We believe this to be because of the absence of nickel coating around the small-scale NdFeB magnets during testing. Because such small-scale magnets have a much higher surface/volume ratio than macroscale magnets, the volume of oxidized material can become a large percentage of the total volume at elevated temperatures. As a result, the irreversible losses are much higher for microscale magnets than that of bulk magnets. SmCo magnets are less sensitive to temperature. Hence, the coefficient for microscale SmCo magnets (α_{SmCo}) is much lower and equals $-0.07\%\,^{\circ}\mathrm{C}^{-1}$ over a wide range of temperatures (25–375 °C).

Fig. 3 shows the measured saturation magnetization of both FeCoV (Hiperco 50) and NiFeMo (Moly Permalloy) as a function of temperature normalized to their respective room temperature values. The magnetic saturation of FeCoV is reasonably stable up to 375 °C, while the saturation magnetization of NiFeMo drops off by more than 60%.

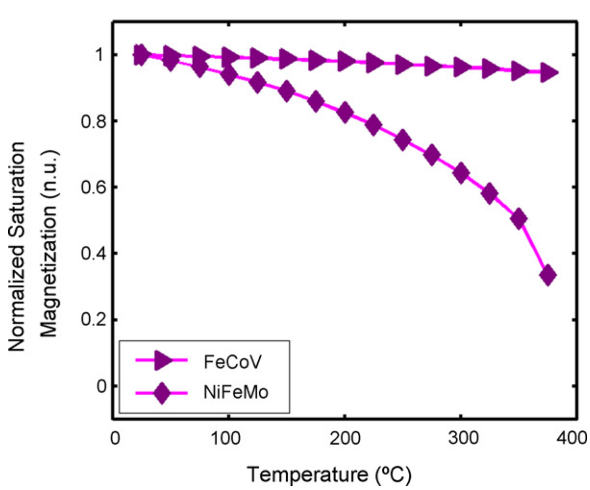

Fig. 3. Measured saturation magnetization of FeCoV and NiFeMo bulk as a function of temperature, normalized to their respective measured room temperature saturation magnetizations. The applied field is 10 kOe.

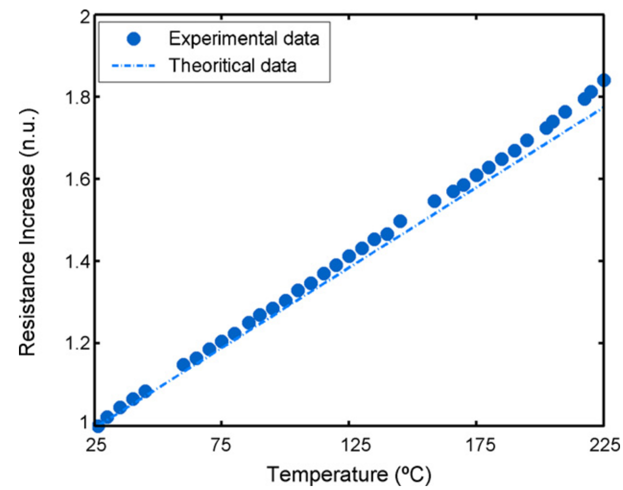

Fig. 4. Measured and theoretical copper winding resistance as a function of temperature, normalized to the room temperature resistance value ($R_{25\,^{\circ}\mathrm{C}} = 172\,\mathrm{m}\Omega$).

4.2. Electrical characterization

The copper winding resistance has been assessed as a function of temperature using a four-point measurement system. The two-layer stator coils are electroplated on a 1 mm thick NiFeMo substrate using conventional microfabrication approaches. The total thickness of the fabricated windings is approximately 200 μm. In practice, the stator is placed on a hotplate, and the resistance variation of a single phase of the 3-phase stator coils is measured as a function of temperature, which is monitored by the digital controller of the hotplate and a thermocouple placed on top of the winding substrate. At room temperature, the single-phase winding resistance ($R_{25\,^{\circ}\mathrm{C}}$) is about 172 mΩ. In the first approximation, experimental data exhibit a linear dependence of copper winding resistance with temperature, and are slightly higher than theory, as presented in Fig. 4. The winding resistance at 225 °C is approximately 1.8 times higher than at room temperature. The coefficient of temperature dependence (β) of the stator coils is defined by

$$R(T) = R_{25\,^{\circ}\mathrm{C}} \times (1 + \beta \times (T - 25)) \quad (2)$$

where $R(T)$ is the single-phase winding resistance at a temperature T (°C), and $R_{25\,^{\circ}\mathrm{C}}$ is the resistance at room temperature. As a result, the measured coefficient of temperature dependence of the electroplated copper windings is $0.0042\,^{\circ}\mathrm{C}^{-1}$.

5. High temperature modeling

Calculations of the delivered output power at high temperatures from the above-mentioned magnetics and conductor heating characterizations are performed. The output power at high temperatures can be expressed as a function of the power at room temperature and the temperature-dependent parameters that have been defined previously (i.e., the operating magnetic field and the coil resistance).

First, the output voltage delivered by the machine is proportional to the magnetic flux density established in the machine, which is itself proportional to the remanence of the permanent-magnet material [14]. As a consequence, the temperature-dependent output voltage varies linearly with the temperature-dependent remanence expressed by Eq. (1). Secondly, assuming that power varies as the square of magnetic flux density established in the machine, and inversely as the winding resistance, and further assuming a linear degradation of both properties with temperature as demonstrated in section 4, the temperature-dependent output power can be phenomenologically modeled as

$$P(T) = P_{25\,^{\circ}\mathrm{C}} \times \frac{(1 + \alpha_{\mathrm{PM}} \times (T - 25))^2}{1 + \beta \times (T - 25)} \quad (3)$$

where $P(T)$ is the DC output power at the operating temperature T, $P_{25\,^{\circ}\mathrm{C}}$ is the DC output power measured at room temperature, α_{PM} is the negative coefficient of temperature dependence for the permanent-magnet materials defined by Eq. (1), and β is the coefficient of temperature dependence for the copper windings determined by Eq. (2). Both coefficients are experimentally identified as presented above.

Fig. 5a and b detail the theoretical power degradation of SmCo and NdFeB microgenerators as a function of temperature. The sole contribution of each material (i.e., copper windings, and PM materials) is also represented. In this regards, the contribution of the stator winding resistance is calculated by assuming that the PM material is not subjected to high temperatures. Similarly, power losses that are exclusively attributable to the permanent magnets are calculated by assuming no temperature-dependent losses of the stator coils.

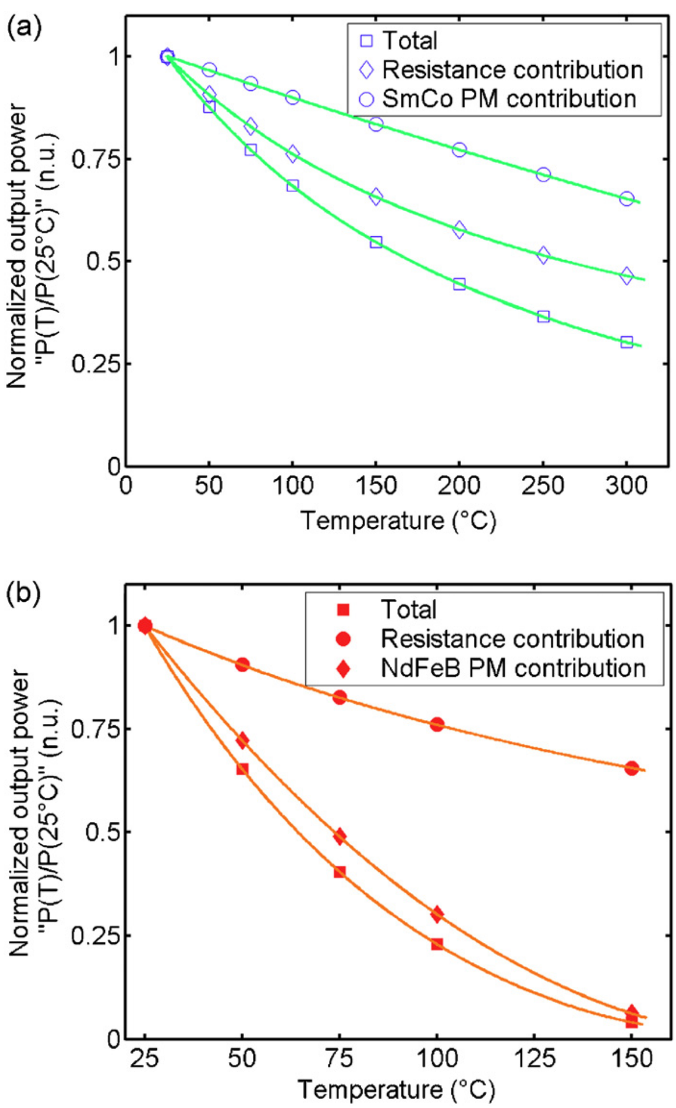

Fig. 5. Theoretical temperature-related power degradation for (a) SmCo microgenerators, and (b) NdFeB microgenerators. The sole contribution of each material (i.e., copper windings, permanent magnet materials) is also represented.

Because the practical air gap between the rotor and stator is small (~100 μm), it is experimentally impossible to isolate and measure separately the temperature-related power degradation caused by each material. However, such analysis emphasizes different behaviors for the two microgenerators. While the power degradation of SmCo machines at high temperatures is dominated by the coil resistance increase, the temperature-related power losses of NdFeB generators are mainly due to the drop of residual magnetization of NdFeB.

6. Power generation

Direct heating experiments of operational microgenerators have been conducted up to 100 °C. Shown in Fig. 6a, a custom 15 mm inner diameter heater has been fabricated, and consists of a copper wire wound around a copper ring. A current source is connected to the copper wire, and temperature is measured using a conventional thermocouple. This heater is used to selectively heat the stator and the rotor, without affecting the plastic turbine blades and ball bearings of the turbine drill. Note that the copper wire is wound and counter-wound to avoid induced fields in the heater region that would corrupt the performance of the generator. Uniform temperatures of up to 100 °C have been achieved inside the oven itself. A rendering of the experimental configuration setup is depicted in

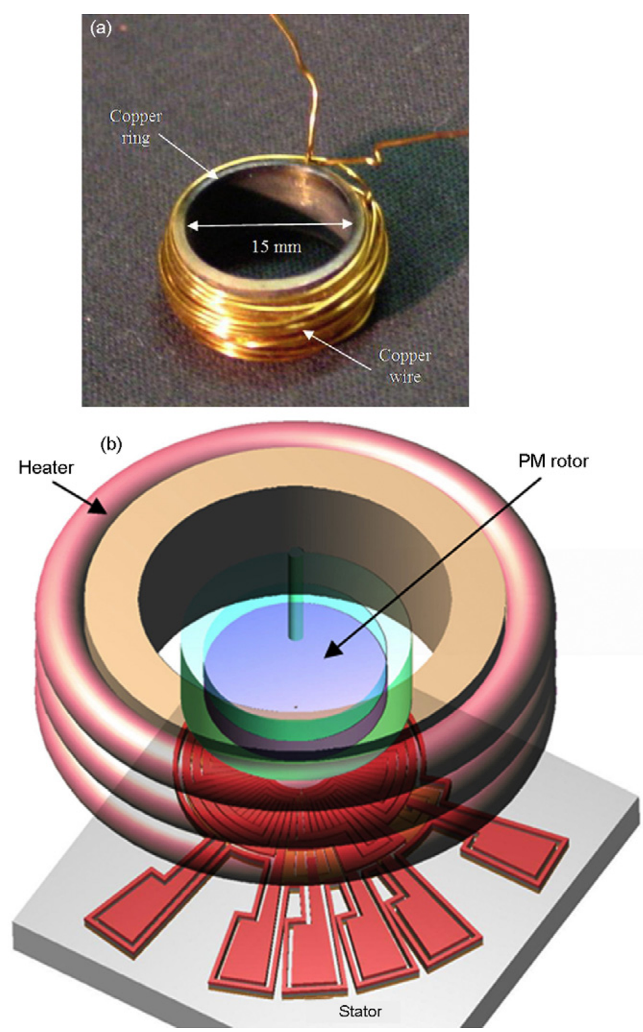

Fig. 6. (a) View of the custom oven for localized heating of rotor and stator, and (b) 3-D rendering of the experimental configuration setup.

Fig. 6b. A commercially available Kapton insulated flexible heater, which consists of a copper coil encapsulated between two layers of Kapton films, is also used underneath the stator substrate to ensure a uniform level of temperature within the substrate. Such heaters are rated up to 200 °C. The operating temperature is monitored by a thermocouple placed inside the custom oven.

For power measurements, the air gap between the stator and the rotor is set at 100 μm. A passive AC/DC converter is used to provide DC power to a resistive load [8]. It should be noted the power converter is separate from the generator and maintained at room temperature. The converter includes a three-phase Δ/wye-connected transformer (1:6 turn ratios) that steps up the AC output voltages, and a three-phase diode bridge rectifier to convert the 3-phase AC signal to a DC output. To minimize the effects of the Schottky diode voltage drops (~0.3–0.4 V), the stator windings are connected in a wye configuration, and coupled to the Δ-connected primary side of the transformer, giving an overall step-up ratio of 18. The resistances of the three-phase transformer are about 20 mΩ and 225 mΩ on the primary and secondary sides, respectively [15]. Experimentally, the output power is calculated by measuring the voltage and current across an external load resistance connected to the diode bridge.

Fig. 7a presents measured and calculated DC output power to an external load using a SmCo rotor as a function of speed for several operating temperatures. A maximum output power of 2.7 W is measured at 100 °C and a rotational speed of 200,000 rpm, while the predicted power is approximately 2.9 W. As compared to the 4 W of power generated at room temperature, this represents a 35% drop of power at 100 °C. Neglecting temperature-related saturation effects associated with the back iron, the phenomenological model shows good agreement with experimental data over the temperature range 25–100 °C (the maximum measurement temperature). At 300 °C, a 70% drop of electrical power is predicted for any given speed, as shown in Fig. 7b. For instance, at a rotational speed of 305,000 rpm, the calculated power is 2.4 W at 300 °C, and the measured power is 8 W at room temperature. However, even at such a high temperature, axial-flux, SmCo microgenera-

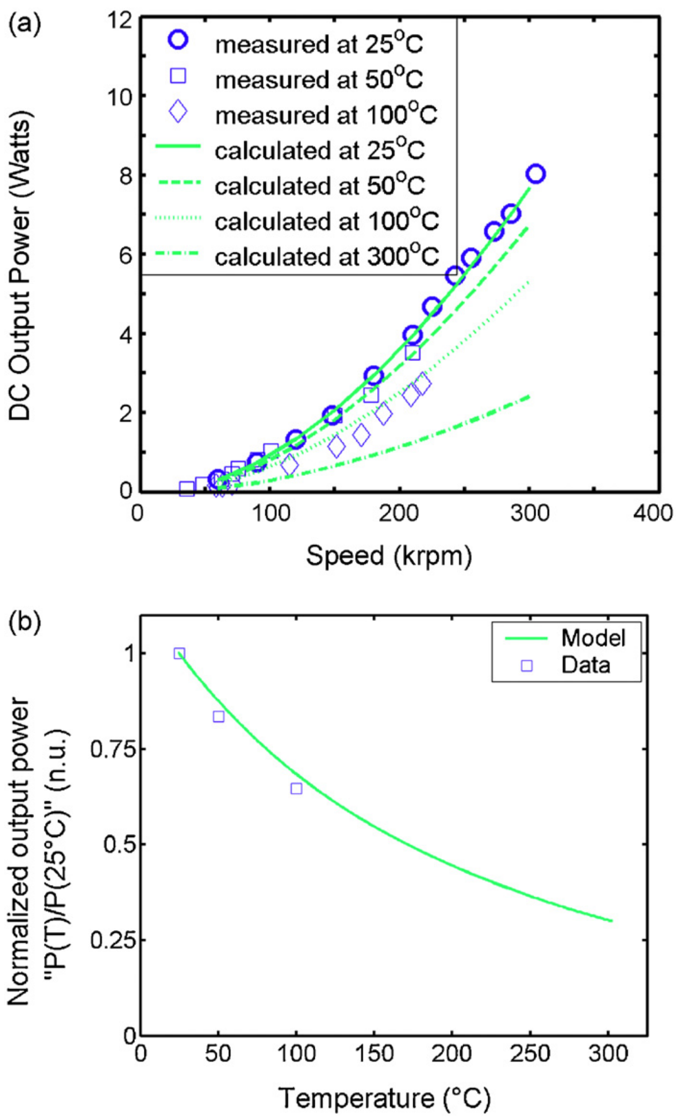

Fig. 7. (a) DC output power measured from a SmCo machine and delivered to external load as a function of speed for several temperatures. The points represent the experimental data, and the lines indicate the calculated output power. (b) DC output power normalized to the room temperature value, as a function of temperature, and for any given speed.

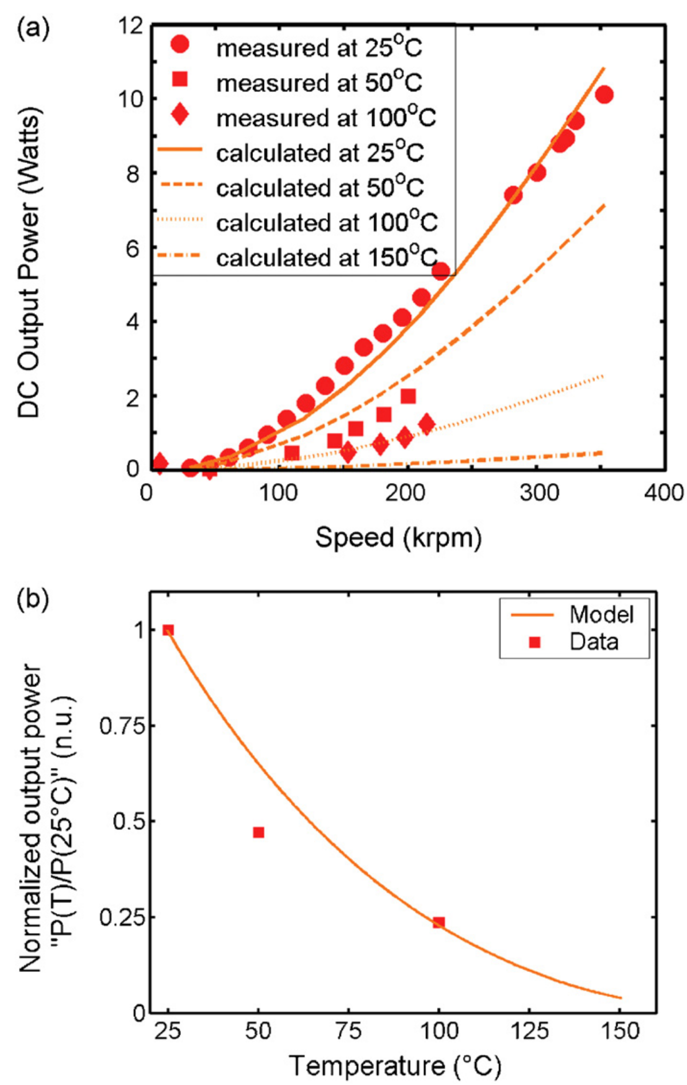

Fig. 8. (a) DC output power measured from a NdFeB machine and delivered to an external load as a function of speed for several temperatures. The points represent the experimental data and the lines indicate the calculated output power. (b) DC output power normalized to the room temperature value, as a function of temperature, and for any given speed.

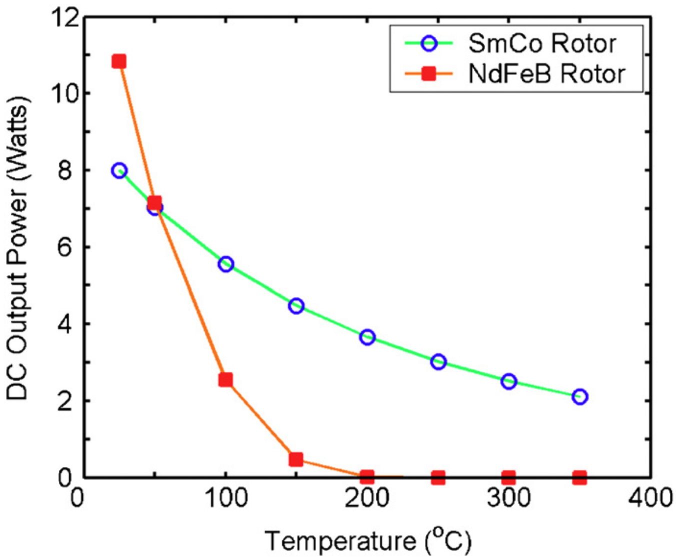

Fig. 9. Calculated DC output power delivered to an external load as a function of temperature for SmCo and NdFeB microgenerators, applying the phenomenological model to the maximum measured output power at room temperature. The rotor speed is assumed to be constant, and at its maximum experimental value (i.e., 305,000 rpm for SmCo rotors, and 400,000 rpm for NdFeB rotors).

tors are still capable of generating appreciable amounts of electrical power.

NdFeB microgenerators have also been tested up to 100 °C. As shown in Fig. 8a, an output power of 1.25 W is achieved across a resistive load at a rotor speed of 215,000 rpm and an external temperature of 100 °C. This corresponds to a 74% drop of output power, as presented in Fig. 8b. While the NdFeB machine outperformed the SmCo machine at room temperature, at 100 °C and 215,000 rpm, the output power delivered by the SmCo machine is twice higher. Furthermore, there is a good agreement between the temperature-dependent model and the experimental data.

Fig. 9 presents the calculated DC output power delivered across a resistive load as a function of temperature for both, SmCo and NdFeB microgenerators, applying the phenomenological model to the maximum measured output power at room temperature. At 25 °C, the highest measured DC output power for NdFeB microgenerators is 10.8 W at a rotational speed of 400,000 rpm. Higher speeds could not be achieved because of the turbine performance. For SmCo microgenerators, a maximum DC output power of 8 W has been measured at 305,000 rpm. At this speed, the rotor suffered catastrophic failure. The power is then calculated as a function of temperature using the phenomenological model previously presented. The assumption that the rotational speeds can remain constant at elevated temperatures is made. Although NdFeB outperforms SmCo in microfabricated generators at room temperature because of higher magnetic performance and higher rotational speeds, NdFeB microgenerators are less efficient than SmCo devices at operating temperatures above 60 °C. High power density, permanent-magnet microgenerators operating in high temperature environment are therefore feasible, and an attractive choice for mechanical-to-electrical converters that are tightly integrated with heat engines.

Future work will focus on high temperature compatible stators, as well as studying further degradation that may occur in the highly stressed, high-speed rotor, caused by deteriorating mechanical properties with temperatures, as well as coefficients of thermal expansion issues.

7. Conclusions

With careful materials selection, MEMS-based permanent-magnet microgenerators capable of multi-watt output power over a wide range of temperatures are feasible. An output power of 2.7 W has been demonstrated at 100 °C for a rotational speed of 210,000 rpm with SmCo rotors. Measurements show a good agreement with a phenomenological model that calculations the power degradation as a function of temperature. Calculations predict that SmCo permanent-magnet microgenerators operating at a temperature of 300 °C are capable of 2.4 W of DC output power across a resistive load at a rotor speed of 300,000 rpm.

Acknowledgements

This work was supported by the United States Army Research Laboratory Collaborative Technology Alliance (DAAD19-01-2-0010). The authors would like to thank Prof. J. Lang and Dr. S. Das of MIT for valuable technical discussions.

References

[1] S.A. Jacobson, A.H. Epstein, An informal survey of power MEMS, in: Proc. Int. Symp. Micro-Mechanical Eng., 2003, pp. 513–520.
[2] H. Raisigel, O. Cugat, J. Delamare, Permanent magnet planar micro-generators, Sens. Actuators A 130–131 (August) (2006) 438–444.
[3] A.S. Holmes, G. Hong, K.R. Pullen, Axial-flux permanent magnet machines for micropower generation, J. Microelectromech. Syst. 14 (February (1)) (2005) 54–62.
[4] D.P. Arnold, F. Herrault, I. Zana, P. Galle, J.-W. Park, S. Das, J.H. Lang, M.G. Allen, Design optimization of an 8-watt, microscale, axial-flux, permanent-magnet generator, J. Micromech. Microeng. 16 (September (9)) (2006) S290–S296.
[5] D.P. Arnold, Y.-H. Joung, I. Zana, J.-W. Park, S. Das, J.H. Lang, D. Veazie, M.G. Allen, High-speed characterization and mechanical modeling of microscale, axial-flux, permanent-magnet generators, in: Proc. Transducers'05, June, 2005, pp. 701–704.
[6] D.P. Arnold, I. Zana, F. Herrault, P. Galle, J.-W. Park, M.G. Allen, Optimization of a microscale, axial-flux, permanent-magnet generator, in: Proc. PowerMems 2005, November, 2005, pp. 165–168.
[7] S. Das, D.P. Arnold, I. Zana, J.-W. Park, M.G. Allen, J.H. Lang, Microfabricated multi-watt permanent-magnet generators – Part I: Modeling, J. Microelectromech. Syst. 15 (October (5)) (2006) 1330–1350.
[8] D.P. Arnold, S. Das, J.-W. Park, I. Zana, J.H. Lang, M.G. Allen, Microfabricated multi-watt permanent-magnet generators – Part II: Design, fabrication, and testing, J. Microelectromech. Syst. 15 (October (5)) (2006) 1351–1363.
[9] I. Zana, F. Herrault, D.P. Arnold, M.G. Allen, Magnetic patterning of permanent-magnet rotors for microscale motor/generators, in: Proc. PowerMEMS 2005, November, 2005, pp. 116–119.
[10] C. Lee, L.G. Frechette, Experimental development of the rotating subsystem for a micro rankine power system, in: Proc. PowerMEMS'05, November, 2005, pp. 37–40.
[11] L.G. Frechette, C. Lee, S. Arslan, Development of a MEMS-based rankine cycle steam turbine for power generation: project status, in: Proc. PowerMEMS'04, November, 2004, pp. 92–95.
[12] S. Stevens, R. Daposhulst, T. Stevens, T. Waumans, R. Van den Braembussche, J. Driesen, J. Piers, R. Belmans, F. Verplaetsen, M. Baelmans, D. Reynaerts, Integrated solution for micro power generation, in: Proc. IEEE Int. conf. on Electric Machines and Drives, May, 2005, pp. 1143–1149.
[13] www.imetra.com.
[14] M.S. Sarma, Electric Machines, second ed., West, New York, 1994, chapters 5, 8.
[15] D. P. Arnold's Thesis, "Magnetic machines for microengine power generation", Georgia Institute of Technology, December 2004.

Biographies

Florian Herrault received the B.S., and M.S. degrees in Physics and Materials Science from the National Institute of Applied Sciences (INSA), Toulouse, France, in 2003 and 2005, respectively. He is currently pursuing his Ph.D. degree in Electrical Engineering from l'Ecole Doctorale de Toulouse, France, at the Georgia Institute of Technology, Atlanta. His Ph.D. research mainly focuses on developing gas-driven, microscale generators. His current research interests include electromagnetic actuators, small-scale power generation systems, and 3-D MEMS fabrication.

David P. Arnold is currently an Assistant Professor in the Department of Electrical and Computer Engineering at the University of Florida, Gainesville. He received dual B.S. degrees in electrical and computer engineering in 1999, followed by the M.S. degree in electrical engineering in 2001, from the University of Florida, Gainesville. He received the Ph.D. degree in electrical engineering at the Georgia Institute of Technology, Atlanta in 2004. As an active member of the Interdisciplinary Microsystems Group at the University of Florida, his research focuses on the design, fabrication, and characterization of magnetically-based microsensors/microactuators, as well as miniaturized power and energy systems. He has co-authored over 35 journal and conference publications, along with one US patent and five patents pending. Dr.Arnold is also a member of IEEE, Tau Beta Pi, Eta Kappa Nu, and the American Society for Engineering Education.

Iulica Zana received the M.S. (1995) degree from The University "Politehnica" of Bucharest, Romania, and the Ph.D. (2003) degree from The University of Alabama, both in Metallurgical and Materials Engineering. He joined Prof. M.G. Allen's group at Georgia Institute of Technology in 2003 as a post-doc, working on developing and implementing magnetic materials into new microfabricated devices. He is now a Principal Engineer with Western Digital. His interests spun across magnetic materials, their deposition and characterization.

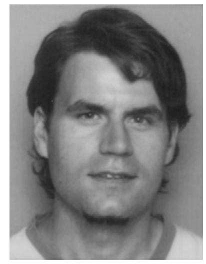

Preston Galle earned a BS degree in Electrical Engineering from Texas A&M University (College Station, Texas) in 1997. He worked as a digital hardware engineer in Portland, Oregon for the proceeding 7 years, the majority of which was divided between a number of startup companies. In 2004, he began studies at the Georgia Institute of Technology (Atlanta, GA), where he is presently working on a Ph.D. thesis combining advances in MEMS, micromagnetics, and power conversion. His additional interests include open source software, robotics, and technology entrepreneurship.

Mark G. Allen (M'89–SM'04) received the B.A. degree in Chemistry, the B.S.E. degree in Chemical Engineering, and the B.S.E. degree in Electrical Engineering from the University of Pennsylvania, Philadelphia, and the S.M. and Ph.D. degrees from the Massachusetts Institute of Technology, Cambridge. Since 1989, he has been with the faculty of the Georgia Institute of Technology (Georgia Tech), Atlanta, where he holds the rank of Regents' Professor in the School of Electrical and Computer Engineering and the J. M. Pettit Professorship in Microelectronics, as well as a joint appointment in the School of Chemical and Biomolecular Engineering. He is also the Senior Vice Provost for Research and Innovation at Georgia Tech. His current research interests are in the field of microfabrication and nanofabrication technology, with emphasis on new approaches to fabricate devices with characteristic lengths in the micro-to nanoscale from both silicon and non-silicon materials. Examples include micromagnetics, high temperature sensors, small-scale power generation, biofluidic microvasculatures and implantable microsensors, and the use of microstructures to create nanostructures. He is North American Editor of the *Journal of Micromechanics and Microengineering*. Dr. Allen was the Cochair of the 1996 IEEE/ASME Microelectromechanical Systems Conference.